PERGAMON

Computers and Structures 77 (2000) 327–342

Computers & Structures

www.elsevier.com/locate/compstruc

A study on crack detection using eigenfrequency test data

Young-Shin Lee*, Myung-Jee Chung

Department of Mechanical Design Engineering, Chungnam National University, Taejon 305-764, South Korea

Received 26 June 1998; accepted 30 June 1999

Abstract

In this paper, a simple and easy nondestructive evaluation procedure is presented for identifying a crack, the location and size of the crack, in a one-dimensional beam-type structure using the natural frequency data. The first procedure is to find the lowest four natural frequencies of the cracked structure by F.E.M. Then, the approximate crack location is obtained by Armon's Rank-ordering method that uses the above four natural frequencies. Second, by applying the result of the crack position range, an appropriate F.E.M. model is adopted and the crack size is determined by F.E.M. Finally, the actual crack location can be identified by Gudmundson's equation using the determined crack size and the aforementioned natural frequencies. The application and accuracy of the proposed procedure can be demonstrated by means of an example of the detection of a crack on the cantilever beam which was tested and studied by Rizos PF, Aspragathos N, Dimarogonas AD. Journal of sound and vibration 1990; 138 (3): 381-388.

Keywords: Crack detection; Eigenfrequency; Crack size; Position; Modal analysis

1. Introduction

Bars and shafts are common structures used to carry and transfer high loads in machines. Cracks are a main cause of structural failure. Sudden failure during high load operation may cause serious damage or injury, so early crack detection is important. Vibration measurements offer a non-destructive, inexpensive and fast means to detect and locate cracks.

The presence of a crack or localized damage in a structure reduces the stiffness and increases the damping in the structure. Vibration theory states, reduction in the stiffness is associated with decrease in the natural frequencies and modification of the modes of vibration of the structure [1].

Many researchers have used one or more of the above characteristics to detect and locate cracks. One of the approaches in detecting damage has been to use changes in the modal parameters, mainly changes in the modal frequencies. With fiber-reinforced plastics, Adams et al. [2] demonstrated that a state of damage can be detected from a decrease in natural frequencies and an increase in damping. Biswas et al. [3] performed experiments on a highway bridge and demonstrated that the decrease in natural frequencies can be used to detect damage. Loland and Dodds [4] used the same principle to detect damage in offshore structures. From relative changes in the natural frequencies of different modes, Loland and Dodds could also predict the location of the damage. Although it is fairly easy to detect the presence of damage in a structure from changes in the natural frequencies, it is difficult to determine the location of the damage. This is because, damage at two different locations may produce the

* Corresponding author.
E-mail address: yslee@shell.chungnam.ac.kr (Y.-S. Lee).

0045-7949/00/$ - see front matter
PII: S0045-7949(99)00194-7

same amount of frequency change as an equal amount of damage in only one location. With the help of analytical beam models, Pandey et al. [5] demonstrated the use of changes in the curvature mode shapes to detect and locate damage. For estimating the location and depth of cracks, Rizos et al. [6] developed a method based on the measurement of amplitudes at two points on the structure vibrating at one of its natural frequencies and an analytical solution of the dynamic response. Gudmundson [7] presented a first order perturbation method which predicts the changes in resonance frequencies of a structure resulting from cracks, notches or other geometrical changes.

Another approach for damage detection, proposed by several researchers, is based on comparing the frequency changes obtained from experimental data collected on the structure with the sensitivity of the modal parameters obtained from an analytical model of the structure. Several researchers have employed different techniques for obtaining this sensitivity, and have also used different methods for comparing experimental results with analytical sensitivities. Using the results of finite element analysis, Cawley and Adams [8] obtained sensitivities of modal parameters and then used the sensitivity values to deduce the location of damage in two-dimensional structures. Based on an analytical model of a fracture-hinge with a rotational spring, Ju and Mimovich [9] developed a modal frequency approach to diagnose fracture damage in simple structures. Inagaki et al. [10] estimated the crack size and position by natural vibration and static deflection analysis, in the case of transverse vibrations of cracked rotors. Qian et al. [11] used a time series technique to estimate the position of a crack on a beam based on a relationship between the crack and the eigencouples (frequencies and mode shapes) of the beam. Shen [12] treated the detection of a crack as an optimization problem in which the crack location and the crack size are estimated by minimizing the difference between the measured frequencies and the frequencies obtained from an analytical analysis of a model for the structure. Kam and Lee [13,14] presented a nondestructive evaluation procedure for identifying a crack in a structure using modal test data based on a simple reduced stiffness model, which can be easily extended to complex structures with multiple cracks.

Another approach in detecting and locating damage has been the use of changes in the structural parameters. Most of the emphasis has been on using changes in the stiffness matrix of the structure.

Park et al. [15] used a stiffness error matrix method based on the difference between analytical stiffness and measured modal properties and, for large stiffness changes, found the method to be successful. To magnify the effect of small stiffness losses on the error matrix, they proposed a weighted-error-matrix method (WEM) which, in addition to changes in the stiffness matrix, utilizes changes in the eigenparameters. Gysin [16] critically evaluated the effectiveness of error matrix methods to locate stiffness change, Mannan and Richardson [17] utilized the difference in the stiffness matrices of intact and damaged structures. Based on governing equations of structural dynamics, Lin [18] has observed that higher modal frequencies contribute to the stiffness matrix values to a greater extent [19].

Among the above studies, Rizos's method [6] using the measured amplitudes at two points of the structure vibrating at one of its natural modes and Kam and Lee's method [14] using the measured vibration frequencies and mode shapes seem to be accurate, simple and easy for crack detection. But these methods need exact measurements for satisfactory accuracy. And especially with Kam and Lee's method [14], crack size can be estimated accurately, but only the approximate crack location can be determined.

In this paper, a simple and easy procedure is presented for determining the crack location and size in a beam-type structure based on only the natural frequency data.

The application and the accuracy of the proposed procedure is demonstrated by means of an example of the detection of a crack on the cantilever beam which was tested and studied by Rizos et al.

2. Theory

2.1. Prediction of crack location

The method to be employed for predicting crack location is Armon's technique [20] utilizing the rank-ordering of the eigenfrequency shifts, which is confirmed by obtaining good agreement between the theoretical and the experimental results. In the following, the theory and technique are introduced.

Crack damage at an element j is represented by reducing the element's stiffness from k_j to k_j^2, $k_j^2 = k_j - \mathrm{d}k$. The mass matrix is assumed to be unaffected by crack damage.

Let the change in the i-th eigenvalue due to a stiffness change $\mathrm{d}k$ at discrete position t be denoted as $\mathrm{d}\omega_i = f(\mathrm{d}k, r)$. Following Cawley and Adams [21] we note that, for small $\mathrm{d}k$, this can be expanded in a Taylor series around $\mathrm{d}k = 0$. Neglecting second and higher-order terms, and noting that $f(0, r) = 0$, we have:

$$\mathrm{d}\omega_i = \frac{\partial f(0, r)}{\partial k}\,\mathrm{d}k = g_i(r)\,\mathrm{d}k \tag{1}$$

which defines the function $g_i(r)$.

In other words, the shift in the eigenfrequency resulting from a single small stiffness change can be expressed as the product of $\mathrm{d}k$ and a function $g_i(r)$, where $g_i(r)$ depends on position but not on magnitude of the stiffness change. This yields the important observation, made by Cawley and Adams, that the ratio of eigenfrequency shifts of two modes depends on the position but not on the magnitude of the stiffness change, for sufficiently small cracks.

Using this result, Armon [20] formulated later a method for identifying the position of a crack without the necessity of simultaneously establishing the magnitude of the crack.

Gladwell's free discrete beam is represented by the matrix formula [20]:

$$Mv(t) + Kv(t) = 0 \tag{2}$$

where M is a diagonal matrix of element masses, K is the stiffness matrix and $v(t)$ is a time dependent vector whose n-th element is the displacement of the n-th mass element. The dots represent differentiation with respect to time. The stiffness matrix for the clamped-free boundary is:

$$K = E\Lambda^{-1}\mathrm{E}\mathrm{K}_0E^{\mathrm{T}}\Lambda^{-1}\mathrm{E}^{\mathrm{T}} \tag{3}$$

where $\Lambda = \mathrm{dia}(l_1,\ldots,l_N,)$ is a matrix of element lengths and $K = \mathrm{dia}(k_1 \ldots k_N)$ is a diagonal matrix of element stiffness. The $N \times N$ matrix E is:

$$E = \begin{vmatrix} 1 & -1 & 0 & \cdots & 0 \\ 0 & 1 & -1 & \cdots & 0 \\ \vdots & \vdots & \vdots & \ddots & \vdots \\ 0 & \cdots & \cdots & 1 & -1 \\ 0 & \cdots & \cdots & 0 & 1 \end{vmatrix} \tag{4}$$

The discrete system, Eq. (2), can be written as an eigenvalue problem:

$$K\bar{v} - \mu M\bar{v} = 0 \tag{5}$$

where μ, $\bar{v}$ are an eigenvalue and eigenvector, respectively. Differentiating this equation with respect to an independent variable s we obtain:

$$(K - \mu M)\frac{\mathrm{d}\bar{v}}{\mathrm{d}s} - \frac{\mathrm{d}\mu}{\mathrm{d}s}M\bar{v} = -\left(\frac{\mathrm{d}K}{\mathrm{d}s} - \mu\frac{\mathrm{d}M}{\mathrm{d}s}\right)\bar{v} \tag{6}$$

Recalling that K and M are symmetrical matrices, the eigenvalue equation can be written:

$$v^{\bar{T}}(K - \mu M) = 0 \tag{7}$$

Multiplying Eq. (6) by $v^{\bar{T}}$ and re-arranging, we obtain

$$\frac{\mathrm{d}\mu}{\mathrm{d}s} = \frac{v^{\bar{T}}\left(\frac{\mathrm{d}K}{\mathrm{d}s} - \mu\frac{\mathrm{d}M}{\mathrm{d}s}\right)\bar{v}}{v^{\bar{T}}M\bar{v}} \tag{8}$$

This equation expresses the change in the eigenvalue as a result of a small change in the independent variables. Let us apply this result to assess the impact of a crack on the eigenfrequencies. This will allow us to assess the eigenfrequency shift due to a small crack, on the basis of knowledge of the crack-free eigenvalues and eigenvectors. As indicated before, a crack is modelled as a reduced stiffness. Thus, we identify it as $\mathrm{d}k$. No change in the mass matrix results from a stiffness change, so $\mathrm{d}M/\mathrm{d}k = 0$.

Consequently, Eq. (8) indicates that the eigenfrequency variation becomes:

$$\frac{\mathrm{d}\mu}{\mathrm{d}k} = \frac{v^{\bar{T}}(\mathrm{d}K/\mathrm{d}k)\bar{v}}{v^{\bar{T}}M\bar{v}} \tag{9}$$

Employ the Rayleigh quotient to express the undamaged eigenfrequencies as:

$$\mu = \frac{v^{\bar{T}}K\bar{v}}{v^{\bar{T}}M\bar{v}} \tag{10}$$

Thus, the fractional variation of the eigenfrequency resulting from a small change $\mathrm{d}k$ in stiffness, becomes:

$$\frac{\mathrm{d}\mu}{\mu} = \frac{v^{\bar{T}}(\mathrm{d}K/\mathrm{d}k)\bar{v}}{v^{\bar{T}}K\bar{v}}\mathrm{d}k \tag{11}$$

Assume a uniform length, l, for all beam elements. Differentiating Eq. (3) with respect to the parameter $\mathrm{d}k$, and replacing non-zero elements of the matrix $\mathrm{d}K/\mathrm{d}k$ in Eq. (11), then we obtain:

$$\frac{\mathrm{d}\mu}{\mu} = \frac{-4(\langle v\rangle - \bar{v}_{n-1})^2}{v^{\bar{T}}K\bar{v}}\mathrm{d}k \tag{12}$$

where $\langle v\rangle$ is defined $\langle v\rangle = (\bar{v}_{n-2} + \bar{v}_n)/2$

It is convenient to convert this expression, based on the discrete flexure model, to a continuous form. To do so, let us note that derivatives of the continuous eigenfunction $u(x)$ are approximated in the discrete model as:

$$\left.\frac{\mathrm{d}u}{\mathrm{d}x}\right|_{x-n} \equiv (\bar{v}_n - \bar{v}_{n-1})/l \tag{13}$$

$$\left.\frac{\mathrm{d}^2u}{\mathrm{d}x^2}\right|_{x=n} \equiv \left[(\bar{v}_n - \bar{v}_{n-1}) - (\bar{v}_{n-2} - \bar{v}_{n-2})/l^2\right] \tag{14}$$

where l is the element length. Recognizing that the denominator of Eq. (12) is proportional to the strain energy, its continuous analog is proportional to $\int_0^L \ddot{u}^2(x)\,\mathrm{d}x$ Thus, the continuous analog of Eq. (12),

for the fractional eigenvalue shifts, is:

$$\frac{d\mu}{\mu} = \beta \frac{\left(d^2u/dx^2\right)}{\int_0^L \left(d^2u/dx^2\right)^2 dx} \tag{15}$$

where β is constant for all modes.

Recall that the eigenvalue μ and eigenfrequency ω are related by β. Fractional eigenfrequency shift as a function of position x/L, is shown in Fig. 1 based on Eq. (15). The values plotted in Fig. 1 have been normalized to unity at $x/L = 0$.

Finally, Fig. 1 can be used to predict the location of the crack with the variation of the rankordering of the eigenfrequency shift in the clamped-beam.

2.2. Finite element analysis

According to the principle of Saint–Venant, the stress field is affected only in the region adjacent to the crack. The element stiffness matrix, except for the cracked element, may be regarded as unchanged under certain limitations of element size. It is very difficult to find an appropriate shape function to express approximately the kinetic energy and elastic potential energy, because of the discontinuity of deformation in the cracked element. Calculation of the additional stress energy of a crack, however, has been studied thoroughly in fracture mechanics and the flexibility coefficient expressed by a stress intensity factor can be easily derived by means of Castigliano's theorem, in the linear–elastic range [11].

A beam finite element with a crack is shown in Fig. 2 [22]. The matrix of linear stiffness of the presented element K_c can be calculated by means of the relationship given by Przemieniecki [23]:

$$K_c = T^T C^{-1} T \tag{16}$$

where $C^{minus;1}$ T is the transformation matrix of a system of the dependent nodes forces $F1$–$F4$ into the independent nodal forces $P1$–$P2$, is the inverse of the flexibility matrix, and superscript T represents the transpose of a matrix.

The form of the transformation matrix T was given by Przemieniecki [23]:

$$T = \begin{Bmatrix} -1 & 1 & 1 & 0 \\ 0 & -1 & 0 & 1 \end{Bmatrix} \tag{17}$$

The flexibility matrix C of the element may be written

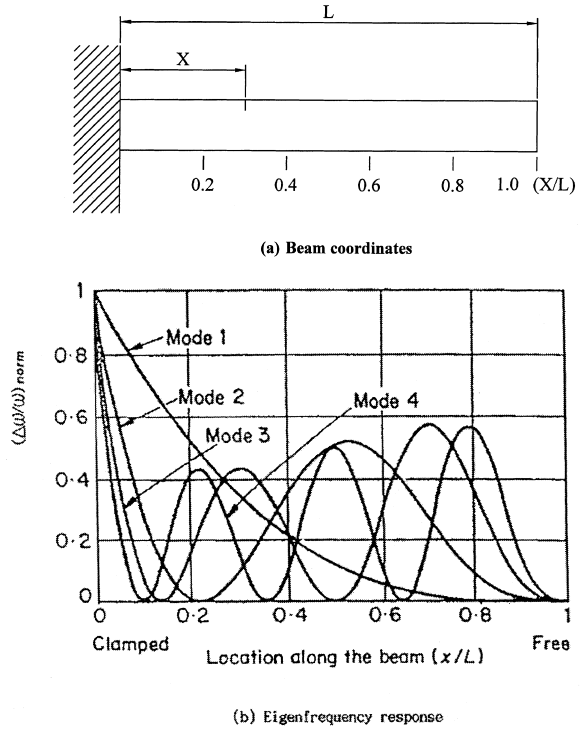

Fig. 1. Fractional eigenfrequency change versus crack position.

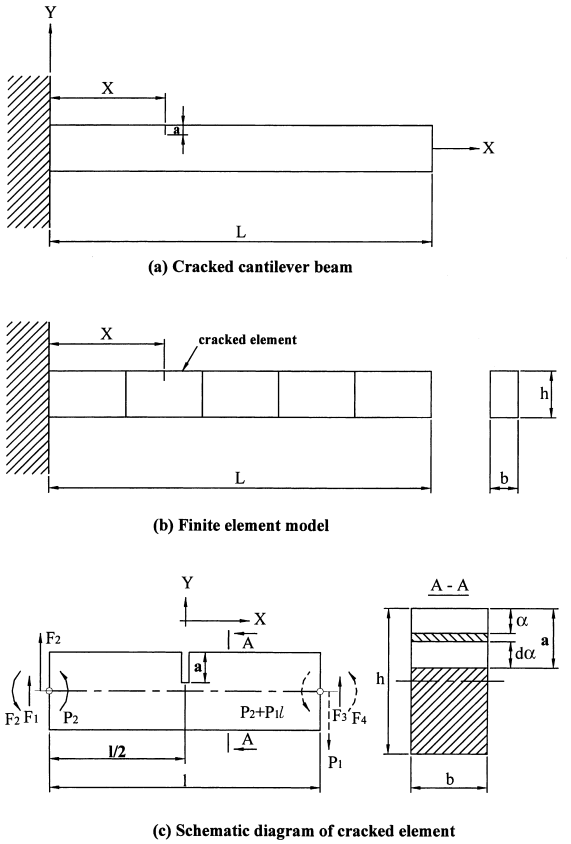

Fig. 2. Cracked cantilever beam and its finite element model.

as the sum of the flexibility matrix C_0 of the uncracked element and the additional matrix C_1 caused by the crack. The terms of the flexibility matrix are calculated by making use of the relationship:

$$C_{ij} = \frac{\partial^2 W_0}{\partial P_i \partial P_j} + \frac{\partial^2 W_1}{\partial P_i \partial P_j} \quad (i = 1, 2; j = 1, 2) \tag{18}$$

where W_0 is the energy of elastic deformation of an uncracked structure and W_1 is the additional energy of elastic deformation caused by the crack.

When shearing is neglected, the energy of elastic deformation of an uncracked beam finite element is equal to:

$$W_0 = \frac{1}{2}\int_0^l \frac{M_b^2}{EI}\,dx \tag{19}$$

where E is Young's modulus, I is the area moment of inertia of the cross-section of the element, l is the length of the element and M_b is the bending moment.

Inserting the following relationship

$$M_b = P_1 X + P_2 \tag{20}$$

into (19), and integrating it with respect to the length of the element, the strain energy of the uncracked element is:

$$W_0 = \frac{P_2^2 l}{2EI} + \frac{P_1 P_2 l^2}{2EI} + \frac{P_1^2 l^3}{6EI} \tag{21}$$

The additional strain energy W_1, due to the crack is described by the following equation [23]:

$$W_1 = \int_A \left[\left(K_I^2 + K_{II}^2\right)/E' + (1+v)K_{III}^2/E\right] dA \tag{22}$$

where A is the area of the crack, $E' = E$ for the state of plane stress. $E' = \frac{E}{(1-v^2)}$, for the state of plane strains, v is Poisson's Ratio. K_I, K_{II}, K_{III} are the stress intensity factors corresponding to the three modes of crack deformation.

Alteration of elastic deformation energy in places of the crack caused by bending moment is the only important change in the case of slender beams. Hence, the relationship (22) for rectangular cross-section given in Fig. 2, and the state of plane strains, may be written in the form:

$$W_1 = \frac{b(1-v^2)}{E}\int_0^a (K_{IM} + K_{IP})^2\,da \tag{23}$$

In this case, the stress intensity factor, K_{IM}, K_{IP} is equal to [24]:

$$K_{IM} = \left(\frac{6P}{bh^2}\right)\sqrt{\pi\alpha}F_I(\bar{\alpha}) \tag{24}$$

$$K_{IP} = \left(\frac{3P_1 l}{bh^2}\right)\sqrt{\pi\alpha}F_I(\bar{\alpha}) \tag{25}$$

where $F_I(\bar{\alpha})$ is the correction function:

$$F_I(\bar{\alpha}) = \sqrt{\frac{\tan(\lambda)}{\lambda}}\frac{0.0923 + 0.199\left[1 - \sin(\lambda)\right]^4}{\cos(\lambda)} \tag{26}$$

where $\alpha = \alpha/h$, $\lambda = \pi\bar{\alpha}/2$, and α, a, b, h are presented in Fig. 2.

Taking into account relations (23) and (24)–(26), W_1 is:

$$W_1 = \frac{\pi(1-v^2)36P_2^2 + 36P_1P_2l + 9P_1^2l^2}{Ebh^2}\int_0^g \bar{\alpha}F_1^2(\bar{\alpha})\,d\bar{\alpha} \tag{27}$$

And taking into account relations (18), (21), (27), the terms of the flexibility matrix of the cracked beam finite element is obtained:

$$c_{11} = \frac{l^3}{3EI} + \frac{18\pi(1-v^2)l^2}{Ebh^2}\int_0^g \bar{\alpha}F_1^2(\bar{\alpha})\,d\bar{\alpha} \tag{28}$$

$$c_{12} = c_{21} = \frac{l^3}{2EI} + \frac{36\pi(1-v^2)l}{Ebh^2}\int_0^g \bar{\alpha}F_I^2(\bar{\alpha})\,d\bar{\alpha} \tag{29}$$

$$c_{22} = \frac{l}{EI} + \frac{72\pi(1-v^2)}{Ebh^2}\int_0^g \bar{\alpha}F_I^2(\bar{\alpha})\,d\bar{\alpha} \tag{30}$$

where $g = a/h$.After performing mathematical operations, we may present the linear stiffness matrix of the cracked beam finite element in explicit form:

$$K_c = \frac{1}{\det C}\begin{vmatrix} c_{22} & c_{22}l - c_{21} & -c_{22} & c_{21} \\ c_{22}l - c_{21} & c_{22}l^2 - c_{31}l - c_{12}l + c_{11} & -c_{22}l + c_{12} & c_{21} - c_{11} \\ -c_{22} & -c_{22}l + c_{21} & c_{22} & -c_{21} \\ c12 & c_{12}l - c_{11} & -c_{12} & c_{11} \end{vmatrix} \tag{31}$$

2.3. Equation of eigenfrequency change

According to the Gudmundson's first order perturbation theory [7], for a small cut-out material, assume that the volume is not changed in the case of a crack, angular eigenfrequency of cracked structure ω_{crack} is:

$$\omega_{crack}^2 = \omega_n^2\left[1 - \frac{W_1}{W_0}\right] \tag{32}$$

where: nth undisturbed angular eigenfrequency:

W_1: additional strain energy due to the crack
W_2: total strain energy in the nth mode of vibration

In the case of cantilever beam such as Fig. 2 considered in this paper, if the Bernoulli–Euler beam theory is used, the total strain energy and angular eigenfrequency of uncracked beam is expressed by:

$$W_0 = \frac{1}{2}A^2 E\frac{\lambda_n^2}{L^4}I_x L \tag{33}$$

$$\omega_n = \frac{\lambda_n^2}{L^2}\sqrt{\left(\frac{EI_x}{\rho S}\right)} \tag{34}$$

where the notation is as listed

A	amplitude of the vibration
L	length of the beam
S	cross-sectional area of the beam
I_x	axial moment of inertia
λ_n	non-dimensional eigenfrequency

Further, λ_n is defined as follows:

$$\lambda_n^2 = 2\pi f_n L^2\sqrt{\frac{\rho A}{EI}} \tag{35}$$

($\lambda_1 \approx 1.8751$, $\lambda_2 \approx 4.6941$, $\lambda_3 \approx 7.8548$, $\lambda_4 \approx 10.9955$ in clamped–free beam [25]). For small cracks, the stress intensity factor of the edge-crack in the beam is the same as for an edge-crack in an infinite half-plane with constant stress

$$K_I = 1.12\sigma\sqrt{\pi a} \tag{36}$$

The strain energy for the crack problem can be computed from the energy release rate.

$$-\frac{\partial U}{\partial a} = \frac{\partial W^1}{\partial a} = b\frac{1-\nu^2}{E}K_I^2 \tag{37}$$

where b represents the thickness of the beam and ν is Poisson's ratio.

An integration of (37) gives the strain energy, W_2^1, as

$$W^1 = b\frac{1-\nu^2}{E}(1.12)^2\sigma^2\pi\frac{a^2}{2} \tag{38}$$

The Bernoulli–Euler beam bending stress can be expressed as follows

$$\sigma = \frac{M_b y}{I} = -E\frac{\partial^2 w}{\partial x^2}y \tag{39}$$

And from the differential equation of the free vibration,

$$EI\frac{\partial^4 w(x,t)}{\partial x^4} + m\frac{\partial^2 w(x,t)}{\partial t^2} = 0 \tag{40}$$

In the case of clamped–free beam, taking into account the boundary condition, the displacement is, [25]

$$w = A\left[\cosh\left(\frac{\lambda_n}{L}x\right) - \cos\left(\frac{\lambda_n}{L}x\right) - k_n\left\{\sinh\left(\frac{\lambda_n}{L}x\right) - \sin\left(\frac{\lambda_n}{L}x\right)\right\}\right] \tag{41}$$

and

$$k_n = \frac{\sin\lambda_n - \sinh\lambda_n}{\cos\lambda_n + \cosh\lambda_n} \tag{42}$$

where A is arbitrary constant, and λ_n is non-dimensional eigenfrequency of Eq. (40).

Eq. (41) substituted into (39) gives

$$\sigma = \frac{h}{2}EA\frac{\lambda_n^2}{L^2}g_n\left(\lambda_n\frac{x}{L}\right) \tag{43}$$

where h is the width of the beam and $g_n(\lambda_n\frac{x}{L})$ is a dimensionless function describing the maximum stress at section x along the beam, and expressed as,

$$g_n = \left[\cosh\left(\frac{\lambda_n}{L}x\right) + \cos\left(\frac{\lambda_n}{L}x\right) - k_n\left\{\sinh\left(\frac{\lambda_n}{L}x\right) + \sin\left(\frac{\lambda_n}{L}x\right)\right\}\right] \tag{44}$$

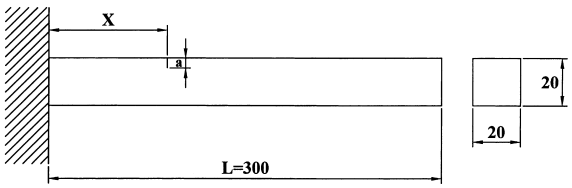

(a) Cracked cantilever beam(mm)

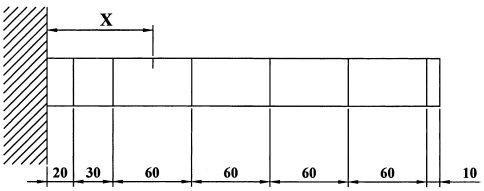

(b) Finite element model(mm)

Fig. 3. Finite element model of cracked cantilever beam for obtaining natural frequencies.

Eqs. (33), (38), (43) introduced into (32) give the new eigenfrequency, $f = \omega/2\pi$, as

$$f^2 = f_n^2\left[1 - 3\pi(1.12)^2(1-\nu^2)\left(\frac{a}{h}\right)\left(\frac{h}{L}\right)g_n^2\left(\lambda_n\frac{x}{L}\right)\right] \tag{45}$$

The non-linear Eq. (45) yields the crack size ratio (a/h) and crack position ratio (x/L), treated as unknowns in the cantilever beam with one edge crack. If the crack size and the natural frequency is determined using the analysis of Section 2.2, the actual crack position can then be determined from Eq. (45) using a Newton–Raphson type iteration method [26].

3. Application

3.1. Analysis model

The aforementioned procedure for crack identification will be applied to detect the location and magnitude of a crack on a cantilever beam. A 300 mm cracked cantilever beam of cross-section 20×20, with modules of elasticity $E = 206$ GPa and mass density $\rho = 7750$ kg/m^3 Fig. 3(a), which was validated by experimental data by Rizos [6] and Kam and Lee [14] has been adopted for this study.

The vibration frequencies of the beam containing edge-cracks of various sizes at different positions along the beam quoted in the reference [14] are given in Table 1.

Table 1
Experimental natural frequencies of cracked cantilever beam

Crack (mm)		Natural frequency		
Position (x)	Depth (a)	Mode 1	Mode 2	Mode 3
10	2	182.7	1149.4	3242.9
	6	163.9	1073.4	3097.3
	10	129.8	980.6	2954.2
80	2	184.0	1160.0	3245.0
	6	174.7	1155.3	3134.8
	10	153.5	1145.1	2934.3
140	2	184.7	1153.1	3258.1
	6	181.2	1092.9	3250.1
	10	171.5	971.5	3233.6
200	2	185.0	1155.0	3238.6
	6	184.3	1106.3	3082.9
	10	182.2	1025.0	2819.6
260	2	185.2	1160.0	3251.1
	6	185.1	1155.1	3193.4
	10	184.9	1139.6	3029.5
No crack	–	185.2	1160.6	3259.1

3.2. Detection of crack

3.2.1. Finite element analysis for natural frequency

Assuming that the natural frequencies in Table 1 are known, to determine the corresponding crack size using the F.E.M. analysis of Section 2.2, the finite element mesh and a cracked element must be considered. Here, these are determined by the method of Rank-Ordering of eigenfrequency shift of Section 2.1.

To apply the Rank-Ordering method using Fig. 1 of the previous section, the natural frequencies from mode 1 to 4 are required. In this report, the natural frequency of mode 4, which was not given in Table 1, is obtained by F.E.M. analysis.

The F.E.M. program used, was made by modifying Reddy's general FEM1D [27] to be able to analyze the modal free vibration and cracked beam element using the stiffness matrix of Section 2.2.

A schematic description of the program algorithm is given in Fig. 4.

The F.E.M. model is shown in Fig. 3(b), in which the crack is located at the mid-span of each cracked element. And to validate the finite element model, the lowest three natural frequencies were compared to the experimental results of Table 1 and to Gudmundson's theory results.

The results are given in Table 2, and the relative natural frequencies (cracked frequency/uncracked frequency) are shown in Figs. 5–8.

As shown in Table 2, the maximum error was no larger than 4%, and in most cases less than 1%,and lower than the Gudmundson's results.

The predicted results for mode 4 natural frequencies obtained from the F.E.M analysis, based on the above validation, are presented in Table 3.

3.2.2. Rank-ordering of modes by fractional eigenfrequency shift

The method for seeking the approximate crack location using Fig. 1 is as follows. Assume that the eigenfrequency shift, ($\Delta\omega/\omega$), is defined as,

$$\Delta\omega/\omega = \frac{\text{uncracked frequency} - \text{cracked frequency}}{\text{uncracked frequency}} \times 100(\%) \tag{46}$$

Let the measured fractional changes of the eigenfrequencies of the first N modes be, $f_1, \ldots, f_N$. Now, arrange these fractional changes in decreasing order:

$$f_{k1} \geq \cdots \geq f_{kN}$$

That is, the mode number f_{k1} has the greatest shift and the mode number f_{kN} has the smallest shift. The rank-ordering of the modes by the fractional eigenfrequency shifts is defined as $k_1, \ldots, k_N$. For example, the rank-

ordering for a crack in the range $0 < x/L < 0.1$ is 1, 2, 3, 4 in Fig. 1.

Table 4 represents crack position range versus rank-ordering of modes when an arbitrary edge crack is contained in a cantilever beam, the value of which can be determined from Fig. 1. The crack position (x/L) is the approximate measured value from the clamped end to the intersection of each mode in Fig. 1. For the model considered in this report, the eigenfrequency shift and the rank-ordering of modes obtained from Tables 1 and 4 is given in Table 5.

Finally, the crack position range determined from Tables 4 and 5 is presented in Table 6.

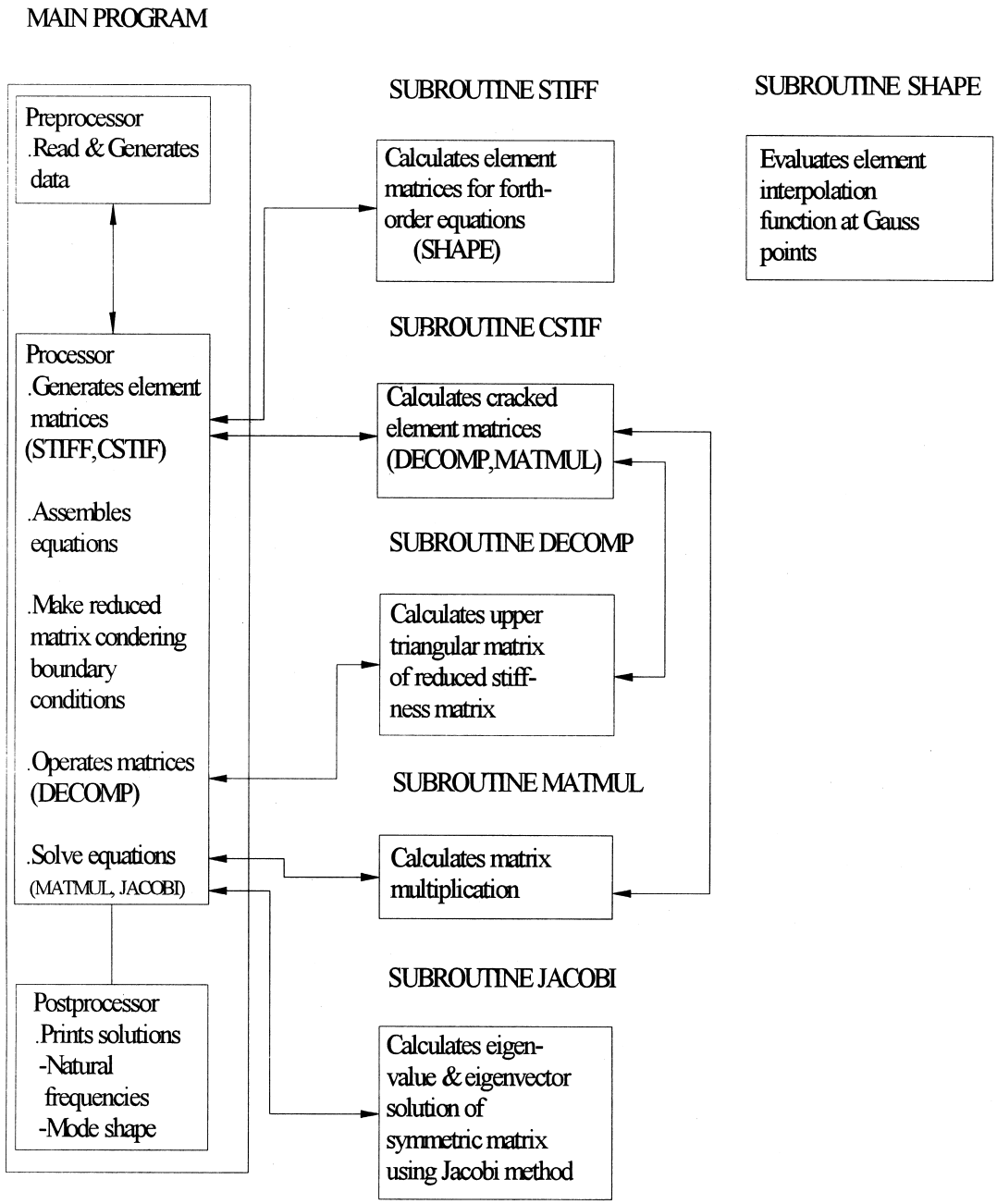

Fig. 4. Structure of the program developed for the modal analysis of one-dimensional cracked beam.

Table 2
Analytical natural frequency comparison with F.E.M. solution and experimental test result[a]

Crack (mm)		Method	Natural frequency (Hz)			Error (%)
Postion (x)	Depth (a)		Mode 1	Mode 2	Mode 3	r.m.s
10	2	Experiment [14]	182.7	1149.4	3242.9	–
		F.E.M.	182.7	1149.2	3234.1	0.16
		Analysis	182.6	1148.0	3222.1	0.38
	6	Experiment [14]	163.9	1073.4	3097.3	–
		F.E.M.	166.9	1083.9	3108.0	1.22
		Analysis	161.9	1048.7	3010.3	2.21
	10	Experiment [14]	129.8	980.6	2954.2	–
		F.E.M.	136.9	996.1	3970.8	3.30
		Analysis	109.0	814.5	3533.9	15.77
80	2	Experiment [14]	184.0	1160.0	3245.0	–
		F.E.M.	184.0	1159.8	3244.9	0.01
		Analysis	184.0	1159.2	3229.7	0.27
	6	Experiment [14]	174.7	1155.3	3134.8	–
		F.E.M.	181.8	1102.9	3250.7	0.56
		Analysis	175.2	1153.9	3082.5	0.98
	10	Experiment [14]	153.5	1145.1	2934.3	–
		F.E.M.	158.4	1147.6	2974.5	2.01
		Analysis	156.0	1143.3	2764.7	3.47
140	2	Experiment [14]	184.7	1153.1	3258.1	–
		F.E.M.	184.7	1153.2	3257.2	0.02
		Analysis	184.7	1151.9	3246.4	0.22
	6	Experiment [14]	181.2	1092.9	3250.1	–
		F.E.M.	181.8	1102.9	3250.7	0.56
		Analysis	181.6	1086.3	3236.6	0.44
	10	Experiment [14]	171.5	971.5	3233.6	–
		F.E.M.	174.0	997.7	3238.0	1.77
		Analysis	175.3	941.3	3216.8	2.23
200	2	Experiment [14]	185.0	1155.0	3238.6	–
		F.E.M.	185.0	1155.0	3238.4	0.01
		Analysis	185.0	1154.1	3223.2	0.28
	6	Experiment [14]	184.3	1106.3	3082.9	–
		F.E.M.	184.4	1114.8	3107.3	0.64
		Analysis	184.4	1106.5	3020.5	1.17
	10	Experiment [14]	182.2	1025.0	2819.6	–
		F.E.M.	182.7	1016.5	2871.0	1.93
		Analysis	183.2	1004.8	2567.6	5.26
260	2	Experiment [14]	185.2	1160.0	3251.1	–
		F.E.M.	185.1	1159.9	3252.1	0.03
		Analysis	185.1	1159.6	3241.5	0.18
	6	Experiment [14]	185.1	1155.1	3193.4	–
		F.E.M.	185.1	1156.2	3204.9	0.22
		Analysis	185.1	1156.3	3191.6	0.07
	10	Experiment [14]	184.9	1139.6	3029.5	–
		F.E.M.	185.0	1145.5	3069.5	0.82
		Analysis	185.0	1149.8	3089.3	1.25
No crack		Experiment (14)	185.2	1160.6	3259.1	
		F.E.M.	185.1	1160.4	3258.1	
		Analysis	185.1	1159.9	3247.7	

[a] r.m.s. Error (%) $= \sqrt{\frac{f_{1\%}^2+f_{2\%}^2+f_{3\%}^2}{3}}$; $f_{N\%} = \frac{f_N - F_{eN}}{f_{eN}} \times 100\%$; f_N = N-mode *cracked natural frequency*; f_{eN}: N-mode *cracked* experimental natural *frequency*.

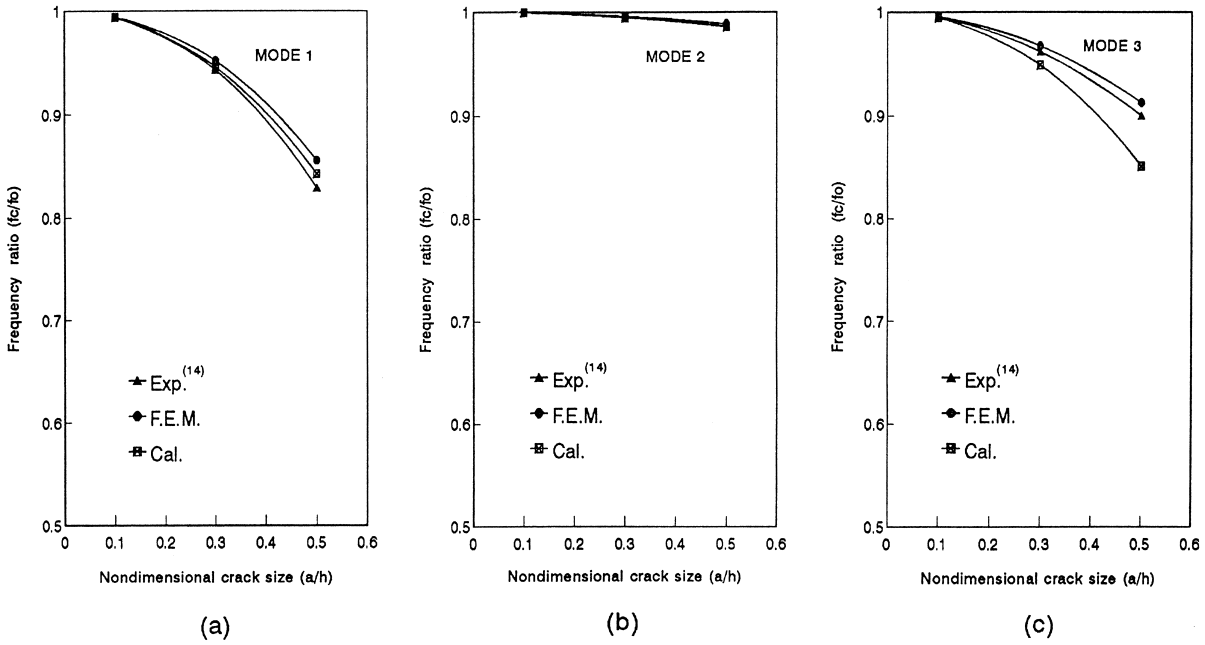

Fig. 5. Comparison of the experimental eigenfrequencies with the F.E.M. and analytical results for crack position $x/L = 0.27$: (a) Mode 1, (b) Mode 2, (c) Mode 3.

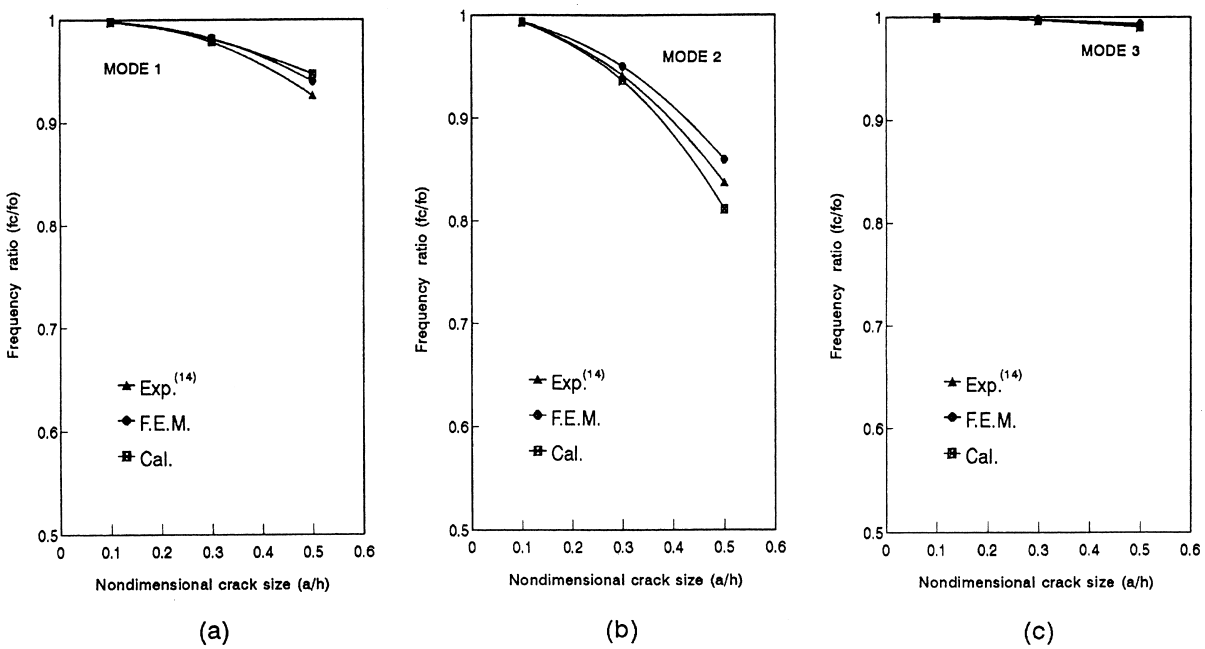

Fig. 6. Comparison of the experimental eigenfrequencies with the F.E.M. and analytical results for crack position $x/L = 0.47$: (a) Mode 1, (b) Mode 2, (c) Mode 3.

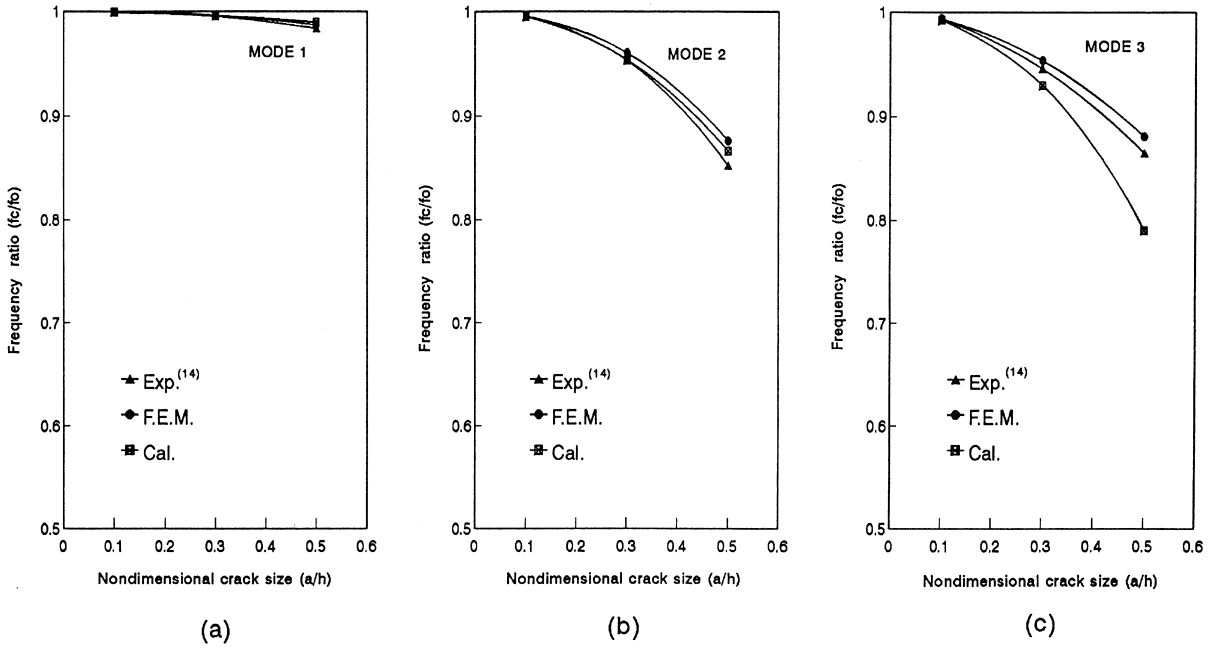

Fig. 7. Comparison of the experimental eigenfrequencies with the F.E.M. and analytical results for crack position $x/L = 0.67$: (a) Mode 1, (b) Mode 2, (c) Mode 3.

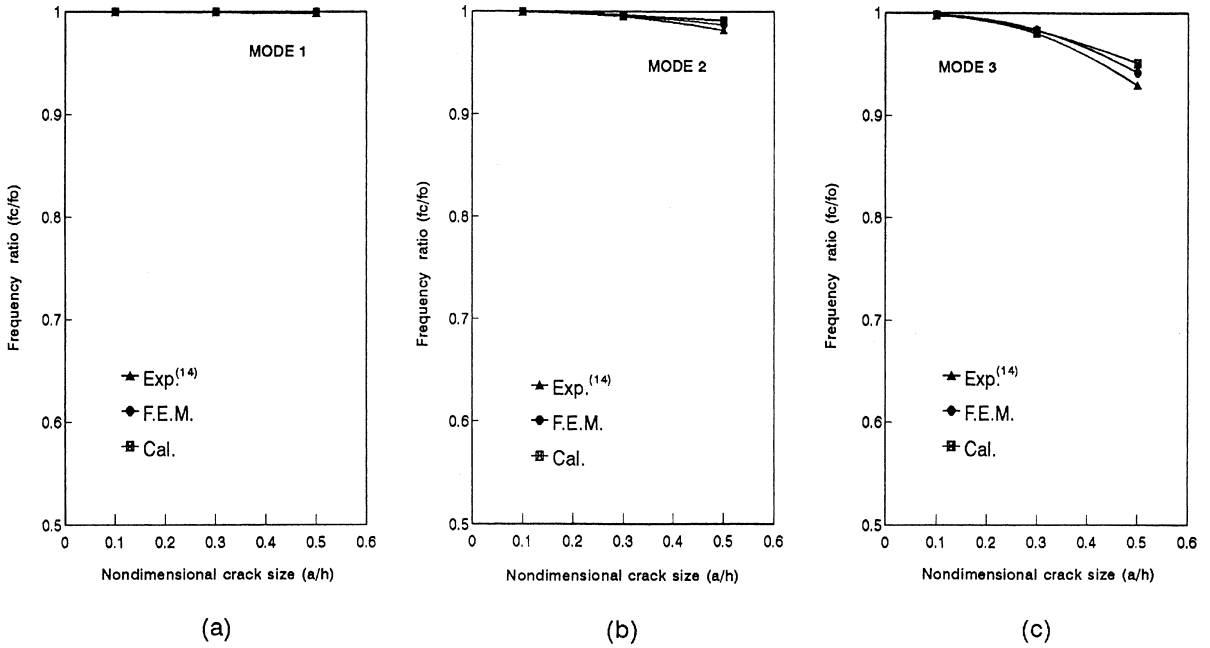

Fig. 8. Comparison of the experimental eigenfrequencies with the F.E.M. and analytical results for crack position $x/L = 0.87$: (a) Mode 1, (b) Mode 2, (c) Mode 3.

Table 3
273Natural frequencies (Mode 4) of cracked cantilever beam by F.E.M. analysis

Crack (mm)		Frequencies (Hz)
Position (x)	Depth (a)	Mode 4
10	2	6405.4
	6	6226.7
	10	6065.9
80	2	6414.8
	6	6300.5
	10	6118.9
140	2	6407.0
	6	6237.3
	10	5942.9
200	2	6430.7
	6	6416.1
	10	6391.8
260	2	6409.6
	6	6235.1
	10	5820.0
No crack		6432.9

Table 4
Crack position range versus rank-ordering of modes from Fig. 1

No.	Crack position range (x/L)	Rank-orde ring of modes
1	0.00–0.11	1234
2	0.11–0.14	1243
3	0.14–0.17	1423
4	0.17–0.25	1432
5	0.25–0.27	1342
6	0.27–0.31	3142
7	0.31–0.36	3124
8	0.36–0.38	3214
9	0.38–0.40	2314
10	0.40–0.41	2134
11	0.41–0.42	2143
12	0.42–0.55	2413
13	0.55–0.59	2431
14	0.59–0.62	2341
15	0.62–0.63	2314
16	0.63–0.67	3214
17	0.67–0.71	3241
18	0.71–0.76	3421
19	0.76–1.0	4321

3.2.3. Estimation of crack depth

Applying the results from Table 6, the F.E.M. model of the beam adopted for crack detection is determined, shown in Fig. 9.

The crack depth can be identified by applying the F.E.M. program which was modified to carry out do-loops in such a way that the natural frequency of the finite element model is equal to the measured value. Here, the natural frequency considered is the lowest one (mode 1), because the crack depth is linear to the frequency at that mode. The crack depth determined by utilizing the procedure is listed in Table 7.

In Table 7, each of the crack numbers 10, 11 and 12 have different crack positions at three crack depths, the correct crack depth will be estimated later. For crack number 13, 14 and 15, mode 2 natural frequency is considered in F.E.M. analysis, because the change of mode 1 frequency at that crack depth was too small for analysis.

Finally, the maximum error for the depth of the crack is 25%, and in most cases less than 8%.

3.2.4. Estimation of crack location

If the depth and natural frequency are determined, the accurate location of the crack can be estimated from Eq. (45) of the previous Section 2.3 using a Newton–Raphson type iteration method. The estimated results are given in Table 8.

In Table 8, the predetermined location of crack numbers 10, 11 and 12, 90–120 mm, is shown to be not acceptable. Therefore, the value of the crack depth in the location must be rejected in Table 7. The results lack accuracy for crack numbers 1, 2 and 3. This can be explained by the fact that for cases when the crack is close to the fixed edge, the predictions are not as good as for other crack positions because the static stress intensity factor will be influenced by the fixation as Gudmundson [7] pointed out.

Considering this fact, if the results determined for crack numbers 1, 2 and 3 that are rejected, the maximum error can be reduced to no larger than 12%, and in most cases 4%. In addition, the error decreases as crack depth becomes smaller.

4. Discussion

Utilizing the present procedure, the cracks have been identified and the results are listed in Tables 9 and 10 with those obtained by Kam and Lee [14] and Rizos [6].

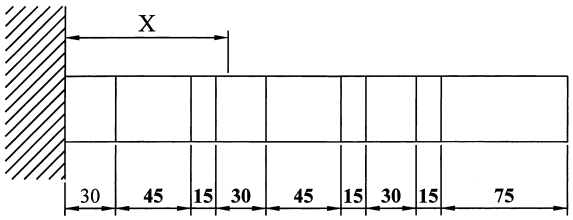

Fig. 9. The scheme of present finite element model of cracked cantilever beam for crack size detection.

Table 5
Eigenfrequency shifts and rank-ordering for cracked beam

Crack no.	Mode 1			Mode 2			Mode 3			Mode 4			Rank
	ω (Hz)	ω_{crack}(Hz)	$\frac{\Delta\omega}{\omega}$(%)	ω(Hz)	ω_{crack}(Hz)	$\frac{\Delta\omega}{\omega}$(%)	ω(Hz)	ω_{crack} (Hz)	$\frac{\Delta\omega}{\omega}$ (%)	ω (Hz)	ω_{crack} (Hz)	$\frac{\Delta\omega}{\omega}$ (%)	
1	185.2	182.7	1.35	1160.6	1149.4	0.97	3259.1	3242.9	0.50	6432.9	6405.4	0.43	1234
2		163.9	11.50		1073.4	7.51		3097.3	4.96		6226.7	3.21	
3		129.8	29.91		980.6	15.51		2954.2	9.36		6065.9	5.71	
4		184.0	0.65		1130.0	0.05		3245.0	0.43		6414.8	0.28	1342
5		174.7	5.67		1155.3	0.46		3134.8	3.81		6300.5	2.06	
6		153.5	17.12		1145.1	1.34		2934.3	9.97		6118.9	4.88	
7		184.7	0.27		1153.1	0.65		3258.1	0.03		6407.0	0.40	2413
8		181.2	2.16		1092.9	5.83		3250.1	0.28		6237.3	3.04	
9		171.5	7.40		971.5	16.29		3233.6	0.78		5942.9	7.62	
10		185.0	0.11		1155.0	0.48		3238.6	0.63		6430.7	0.03	3214
11		184.3	0.47		1106.3	4.68		3082.9	5.41		6416.7	0.26	
12		182.2	1.62		1025.0	11.68		2819.6	13.49		6391.8	0.64	
13		185.2	0.0		1160.0	0.05		3251.1	0.25		6409.6	0.36	4321
14		185.1	0.05		1155.1	0.47		3193.4	2.02		6235.1	3.07	
15		184.9	0.16		1139.6	1.81		3029.5	7.04		5820.0	9.53	

From Tables 9 and 10, it appears that Kam and Lee's method has the best agreement with actual crack depth. But the method adopted the estimation of crack location as the cracked element. Thus, it is reasonable to assume that the accuracy of the present procedure is comparable only to Rizos's method.

Assuming that the maximum error in crack location, 25%, is due to the inaccurately measured frequency, the total error of the present method in crack depth and location is no larger than 12%.

Although the error of the present method is larger than that of Rizos's result (8%) which is based on the two exact modal measured values (mode shape and amplitude), this is not a severe limitation because in most practical structures a 10% crack is not usually an indication of immediate failure.

Considering the general crack detection method by vibration analysis can be used to locate the crack roughly before using the non-destructive testing method such as ultrasonic, radiography, etc., the present method is thought to be a simple and easy one to be able to apply to real structures.

Table 6
Proposed crack position range of cracked beam

Crack no.	Rank	Crack position	
		x/L	x (mm)
1	1234	0.00–0.11	0–33
2			
3			
4	1342	0.25–0.27	75–81
5			
6			
7	2413	0.42–0.55	126–165
8			
9			
10	3214	0.36–0.38 or 0.63–0.67	108–114 or 189–201
11			
12			
13	4321	0.76–1.00	228–300
14			
15			

5. Conclusions

The easiest method for detecting a crack using the lowest four natural frequencies is presented in this study, and applied to a cantilever beam with one edge crack. The following conclusions can be drawn.

1. The maximum error regarding size of the crack is 25%, and it could be less than 8% if the procedure is based on the correct measured values of the natural frequency.
2. The predictions in position of the crack are not as good as for other positions, when the crack is close to the clamped end. The error is no larger than 12%, and in most cases less than 4% in other areas; and it is reduced with decreasing crack sizes.
3. This identification procedure is believed to be an alternative procedure for crack detection, because the difference with Rizos's identified values is not large. Modification in the theory of the crack analy-

Table 7
Comparison of actual and estimated crack depth

Crack no.	Actual crack (mm)		Estimated crack (mm)		Error (%)	
	Position (x)	Depth (a)	Position range	Depth (a)	%[a]	r.m.s[b]
1	10	2	0–30	2.06	3.0	8.32
2		6		6.66	11.0	
3		10		10.88	8.8	
4	80	2	75–90	2.03	1.5	10.33
5		6		6.63	10.5	
6		10		11.44	14.4	
7	140	2	120–150	1.95	−2.5	8.03
8		6		6.62	10.3	
9		10		10.90	9.0	
10	200	2	90–120	–	–	62.14
11		6		2.08	−65.3	
12		10		4.12	−58.8	
10		2	180–210	1.80	−10.0	6.55
11		6		6.03	5.0	
12		10		10.19	1.9	
13	260	2	225–300	1.20	40.0	25.59
14		6		6.83	13.8	
15		10		11.32	13.2	

[a] % Error $= \frac{\text{Estimated value}-\text{Actual value}}{\text{Actual value}} \times 100(\%)$.

[b] r.m.s. Error $+ \frac{\sqrt{E_1^2+E_2^2+E_3^2}}{3}$($E_1$, E_2, E_3: % Error).

Table 8
Comparison of actual and estimated crack position

Crack no.	Actual crack (mm)		Estimated crack (mm)		Error (%)	
	Position (x)	Depth (a)	Position range	Depth (a)	%[a]	r.m.s[b]
1	10	2	0–30	18.47	84.70	84.70
2		6		38.50	–[c]	
3		10		49.42	–[c]	
4	80	2	75–90	82.10	2.63	12.16
5		6		90.21	12.76	
6		10		93.23	16.54	
7	140	2	120–150	138.36	−1.17	3.47
8		6		143.95	2.82	
9		10		132.76	−5.17	
10	200	2	90–120	–	–	–
11		6		447.37	–[c]	
12		10		445.38	–[c]	
10		2	180–210	193.25	−3.38	4.19
11		6		195.60	−2.20	
12		10		187.93	−6.04	
13	260	2	225–300	–	–	1.54
14		6		259.77	−0.09	
15		10		254.32	−2.18	

[a] % Error $= \frac{\text{Estimated value}-\text{Actual value}}{\text{Actual value}} \times 100(\%)$.

[b] r.m.s. Error $+ \frac{\sqrt{E_1^2+E_2^2+E_3^2}}{3}$($E_1$, E_2, E_3: % Error).

[c] Data not available.

Table 9
Actual and estimated crack position with various methods

Actual crack (mm)		Estimate crack(mm)							
		Present method			Kam and Lee's method [14]	Rizos's method [6]			
Position (x)	Depth	Position (x)	Error		Position (x)	Position (x)	Error		
			%[a]	r.m.s[b]			%	r.m.s	
10	2	18.47	84.70	84.70	0–50	10.31	3.00	2.94	
	6	–	–			9.92	−1.00		
	10	–	–			10.41	4.00		
80	2	82.10	2.63	12.16	50–110	78.61	1.75	2.66	
	6	90.21	12.76			80.93	1.12		
	10	93.23	16.54			83.31	4.12		
140	2	138.36	−1.17	3.47	110–170	138.72	−0.92	2.34	
	6	143.95	2.82			139.41	−0.42		
	10	132.76	−5.17			145.51	3.92		
220	2	193.25	−3.38	4.19	170–230	200.72	0.35	3.01	
	6	195.60	−2.20			200.13	0.05		
	10	187.93	−6.04			210.43	5.20		
260	2	–	–	1.54	230–300	275.81	6.07	7.68	
	6	259.77	−0.09			235.22	−9.54		
	10	254.32	−2.18			278.22	7.00		

[a] $\%\ \text{Error} = \frac{\text{Estimated value} - \text{Actual value}}{\text{Actual value}} \times 100(\%)$.

[b] $\text{r.m.s. Error} = \frac{\sqrt{E_1^2 + E_2^2 + E_3^2}}{3}(E_1, E_2, E_3 : \%\ \text{Error})$.

Table 10
Actual and estimated crack position with various methods

Actual crack (mm)		Estimated crack (mm)								
		Present method			Kam and Lee's Method [14]			Rizos's method [6]		
Position (x)	Depth (a)	Depth (a)	Error		Depth (a)	Error		Depth (a)	Error	
			%	r.m.s		%	r.m.s		%	r.m.s
10	2	2.06	3.00	8.32	1.96	−2.00	1.18	2.08	4.00	3.43
	6	6.66	11.00		6.02	0.33		5.89	−1.83	
	10	10.88	8.80		10.03	0.30		10.40	4.00	
80	2	2.03	1.50	10.33	1.87	−6.50	3.75	1.95	−2.50	3.55
	6	6.63	10.50		6.01	0.17		6.32	5.33	
	10	11.44	14.40		10.01	0.10		9.82	−1.80	
140	2	1.95	−2.50	8.03	2.02	1.00	0.61	1.91	−4.50	4.79
	6	6.62	10.33		5.99	0.10		6.38	6.33	
	10	10.90	9.00		10.03	0.30		9.71	−2.90	
200	2	1.80	– 10.00	6.55		1.00	0.60	2.10	5.00	5.76
	6	6.03	5.00		6.01	0.17		5.60	−6.66	
	10	10.19	1.90		9.98	−0.20		9.45	5.50	
260	2	1.20	40.00	25.59	2.07	3.50	2.02	2.13	6.50	5.71
	6	6.83	13.80		6.01	0.17		5.38	−2.83	
	10	11.32	13.20		10.01	0.10		9.31	−6.90	

sis must be made, if the present procedure is extended to the identification of multiple cracks.

References

[1] O'Brian TK. In: Mechanics of Non-Destructive Testing. New York: Plenum Press, 1980. p. 101–21.

[2] Adams RD, Short D. Vibration testing as a nondestructive test tool for composite materials. ASTM STP 1975;580:159–75.

[3] Biswas M, Samman MM. Diagnostic experimental spectral/modal analysis of a highway Bridge. The International Journal of Analytical and Experimental Modal Analysis 1990;1:33–42.

[4] Loland O, Dodds CZ. Experiences in developing and operating integrity monitoring system in North Sea. Proceedings of the 8th Annual Offshore Technology Conference 1976;2:313–9.

[5] Pandey AK, Samman MM. Damage detection from changes in curvature mode shapes. Journal of Sound and Vibration 1991;145(2):321–32.

[6] Rizos PF, Aspragathos N, Dimarogonas AD. Identification of crack location and magnitude in a cantilever beam from the vibration modes. Journal of Sound and Vibration 1990;138(3):381–8.

[7] Gudmundson P. Eigenfrequency changes of structures due to cracks, notches or other geometrical changes. Journal of Mechanics and Physics of Solids 1982;30:339–53.

[8] Cawley P, Adams RD. The location of defects in structures from measurements of natural frequencies. Journal of Strain Analysis 1979;14:49–57.

[9] Ju FD, Mimovich M. Modal frequency method in diagnosis of fracture damage in structures. Proceedings of the 4th International Modal Analysis Conference 1986;2:1168–74.

[10] Inagaki T, Shiraki K. Transverse vibrations of a general cracked rotor bearing system. Trans of ASME, Journal of Mechanical Design 1981;104:1–11.

[11] Qian GL, Gu SN, Jiang JS. The dynamic behaviour and crack detection of a beam with a crack. Journal of Sound and Vibration 1990;138(2):233–43.

[12] Shen, M.H.H., 1989. Natural modes of cracked beams and identification of cracks, Ph.D. Dissertation presented to the University of Michigan, Ann Arbor, MI.

[13] Lee TY, Kam TY. Detection of crack location via a global minimization approach. Engineering Optimization 1993;21:147–59.

[14] Kam TY, Lee TY. Detection of cracks in structures using modal test data. Engineering Fracture Mechanics 1992;42:381–7.

[15] Pak YS, Lee SS. Weighted-error-matrix application to detect stiffness damage by dynamic-characteristic measurement. International Journal of Analytical and Experimental Modal Analysis 1998;3:101–7.

[16] Gysin HP. Critical application of the error matrix method for localisation of finite element modelling inaccuracies. Proceedings of the 4th International Modal Analysis Conference 1986;2:1339–51.

[17] Mannan MA, Richardson MH. Detection and location of structural cracks using FRF measurements. Proceedings of the 8th International Modal Analysis Conference 1990;1:652–7.

[18] Lin CS. Location of modeling errors using modal test data. AIAA Journal 1990;28:1650–4.

[19] Pandey AK, Biswas M. Damage detection in structures using changes in flexibility. Journal of Sound and Vibration 1994;169(1):3–17.

[20] Armon D, Ben-Haim Y, Braun S. Crack detection in beams by rank-ordering of eigenfrequency shift. Mechanical Systems and Signal Processing 1994;8:81–91.

[21] Adams RD, Cawley CJ. A vibration technique for nondestructively assing the integrity of structures. Journal of Mechanical Engineering Sciences 1978;20:93–100.

[22] Krawczuk M, Ostachchowicz WM. Transverse natural vibration of a cracked beam loaded with a constant axial force. Trans of the ASME Journal of Vibration and Acoustics 1993;115(4):524–8.

[23] Przemieniecki JS. Theory of Matrix Structural Analysis. New York: McGraw Hill, 1968.

[24] Tada H, Paris P, Irwin G. The Stress Analysis of Cracks Handbook. Hellertown, Pennsylvania: Del Research Corporation, 1973.

[25] Blevins RD. Formulas for Natural Frequency And Mode Shape. New York: van Nostrand Reinhold, 1979.

[26] Kuo SS. Computer Applications of Numerical Methods. Reading, MA: Addison–Wesley, 1972.

[27] Reddy JN. An Introduction to the Finite Element Method. New York: McGraw Hill, 1984.